ELASTIC-PLASTIC FRACTURE TOUGHNESS TESTS WITH SINGLE-EDGE NOTCHED BEND SPECIMENS*

T. L. Anderson[1], H. I. McHenry[1], M. G. Dawes[2]

[1] Fracture and Deformation Division
National Bureau of Standards
Boulder, Colorado 80303

[2] The Welding Institute
Abington Hall
Abington, Cambridge
CB1 6AL, England

Submitted for inclusion in the proceedings of the Symposium on User's Experience with Elastic-Plastic Fracture Toughness Test Methods.

ABSTRACT

Fracture toughness tests have been performed on five geometries of single-edge notched bend (SENB) specimens machined from a 25.4-mm (1.0-in) thick plate of normalized steel. Critical values of the J-integral and the crack-tip opening displacement (CTOD) were measured as a function of temperature. Test temperatures, which ranged from -196°C to 25°C, covered the entire ductile-to-brittle transition range. On the upper shelf, critical values of J and CTOD at the onset of stable crack growth were insensitive to specimen geometry. However, in the ductile-to-brittle transition region, where fracture occurred by unstable cleavage, fracture toughness decreased with increasing specimen thickness and crack length. This effect of geometry on fracture toughness in the transition region is attributed to changes in crack-tip region constraint with geometry.

Various aspects of the SENB fracture toughness test have been examined. Experimental results indicate that both J and CTOD can be accurately measured with a single clip gage. Work hardening caused the ratio of J to CTOD to increase with strain. The m factor, which relates J to CTOD and flow stress, was directly proportional to the notch constraint factor. The n factor, which is a dimensionless constant used to relate the J-integral to energy absorbed by the specimen, was independent of crack length for SENB specimens with a/W ranging from 0.19 to 0.75. The rotational factor, r_p, was not a strong function of temperature or specimen geometry.

Key Words: Crack-tip opening displacement; ductile-to-brittle transition; elastic-plastic fracture; J-integral; mechanical properties; structural steels; toughness.

Structural steels undergo a transition from fully ductile to fully brittle behavior as temperature is decreased. Lower shelf (brittle) fracture behavior can be quantified by K_{Ic}, and upper shelf (ductile) fracture resistance can be described in terms of J_{Ic}. Both J_{Ic} and K_{Ic} are material properties that are independent of the geometry of the test specimen or structure. Fracture in the ductile-to-brittle transition region usually occurs by unstable cleavage but extensive plastic flow at the crack tip can occur prior to failure. This crack-tip plasticity invalidates a description of the fracture resistance in terms of K_{Ic}. Thus, fracture in the transition region must be addressed with elastic-plastic analyses. However, the J_{Ic} test method as defined in ASTM Standard E 813 is only valid for upper shelf behavior. The crack-tip opening displacement (CTOD) test [1] is the only standardized test that covers all fracture behaviors that can occur between the extremes associated with the K_{Ic} and J_{Ic} tests. Recently, Dawes [2] has proposed a J equivalent of the CTOD test. This would give the same continuity in J-based tests as in CTOD-based tests.

Contrary to common assumptions, there is not, at present, a geometry-independent fracture toughness parameter for the ductile-to-brittle transition region of steels. Data of various investigators indicate that critical values of J and CTOD in the transition region are affected by the geometry of the fracture specimens [3-12]. Larger specimens tend to induce a greater degree of stress triaxiality near the crack tip, thereby limiting plastic flow. This constraint of plastic flow is believed to be responsible for shifting the ductile-to-brittle transition to higher temperatures.

This paper presents experimental data that show the effect of geometry of single-edge notched bend (SENB) specimens on critical J and CTOD values in the ductile-to-brittle transition region. In addition, various aspects of

elastic-plastic fracture toughness tests with SENB specimens are analyzed. The topics discussed include: relationships between J and CTOD, measurement of both J and CTOD with a single clip gage, and detecting the onset of tearing in an SENB specimen.

The major advantage of the SENB specimen (see Fig. 1) over the compact tension (CT) specimen is its relatively low machining cost. Also, the SENB specimen has lower load requirements than a CT specimen with the same ligament dimensions. An SENB specimen with the desired notch location and orientation can be more readily machined out of a welded plate and therefore it is better suited to fracture toughness testing of weldments. Also, one can make simultaneous measurements of J and CTOD during a fracture test with an SENB specimen; there is presently no standardized test method for measuring the CTOD of a CT specimen.

TEST MATERIAL

The test material was a 25.4-mm (1.0-in) thick plate of ABS grade EH36 steel, a 350-MPa (51-ksi) yield strength carbon-manganese steel whose chemical composition is given in Table 1. The steel was in the normalized condition and had particularly uniform properties because of sulfide shape control.

The tensile properties of the normalized steel were determined from round tensile specimens (6.35-mm diameter and 31.75-mm gage length) with the tensile axis parallel to the rolling direction. These specimens were tested at various temperatures ranging from -196°C to 25°C. All tensile tests were performed in a screw-driven tensile test machine at a crosshead speed of 0.2 cm/min. All testing and measurement procedures conformed to the guidelines of ASTM E 8, the standard for tensile testing of metals.

The tensile properties as a function of temperature are shown in Fig. 2. The data followed the expected trends with a minimal amount of scatter. Both the yield strength and the ultimate tensile strength increased markedly with decreasing temperature. All flow curves exhibited an upper and lower yield point, which is characteristic of low-carbon steels. The yield strength (as plotted in Fig. 2) was defined as the upper yield point; this definition was used to conform to the specifications of ASTM E 8.

EXPERIMENTAL PROCEDURE

The ductile-to-brittle transition curves have been established as a function of constraint in SENB specimens. Notch constraint was varied by varying the crack-length/width ratio, a/W, and the specimen thickness, B. The fracture toughness test matrix is shown in Table 2. The specimens were machined with the notch orientation shown in Fig. 3.

All specimens were fatigue-precracked at room temperature according to the specifications in the British Standard for COD testing [1]. The tests were performed in displacement control on a 100-kN servohydraulic test machine. The displacement rate in all tests was 0.80 mm/min. The mouth-opening displacement and the load-line displacement were measured simultaneously during the test by two clip gages. The load-line displacement was measured by the comparison bar technique developed by Dawes [13]. The load and the two displacements were recorded on a two-pen X-Y plotter. The test instrumentation was wired to a minicomputer through an analog-to-digital converter. The load, crosshead displacement, and both clip-gage displacements were recorded by the computer at approximately 0.3-s intervals and stored on a magnetic disk. The computer typically collected and stored around 500 sets of data in a 3- to 5-minute bend test.

Low temperatures were attained by attaching a box to the lower crosshead and filling it with either liquid nitrogen or an alcohol and dry ice mixture. Intermediate temperatures (between -196 and -70°C) were attained by pouring liquid nitrogen into the box to a level below the specimen. The specimen was cooled by heat transfer through the test fixture and by the vapor coming off of the boiling nitrogen below the specimen. The actual specimen temperature was measured by a thermocouple implanted in the specimen.

In each test, fracture toughness was measured by the two elastic-plastic fracture parameters, J and CTOD. Figure 4 shows the notation used for critical values of CTOD [1]. The notation depends on the nature of the fracture event, i.e., whether the crack extension is brittle or ductile, and whether or not unstable cleavage is preceded by stable crack growth. A similar notation is used for reported critical values of the J-integral [2] (see Fig. 5).

CTOD was computed from the following relationship:

$$\delta = \delta_e + \delta_p = \frac{K^2}{2\sigma_o E} + \frac{r_p(W-a)\, V_p}{r_p(W-a) + a + z} \qquad (1)$$

where V_p = plastic component of the mouth-opening displacement

z = knife edge thickness

r_p = rotational factor

σ_o = yield stress

K = stress intensity factor

E = Young's modulus

This equation separates CTOD into elastic and plastic components (δ_e and δ_p). The British Standard [1] suggests that a value of 0.4 be assumed for r_p in Eq 1. However, a more precise value for the rotational factor can be calculated if the plastic components of load-line displacement and mouth-opening displacement (q_p and V_p, respectively) are known [14]:

$$r_p = \frac{1}{W-a} \frac{V_p W}{q_p} \left(1 - \frac{q_p}{16\,W}\right) - (a + z) \qquad (2)$$

The average value of r_p was found to be $\sim$0.5 for this specimen material (see Results and Discussion Section). This value was used in Eq 1 for all CTOD calculations.

The ASTM Standard E 813, the standard for J_{Ic} testing, recommends that the following equation be used to estimate the J-integral for an SENB specimen:

$$J = \frac{2U}{B(W-a)} \qquad (3)$$

where U is the area under the load/load-line displacement curve. However, J can also be estimated from an equation derived by Sumpter and Turner [15]:

$$J = \frac{K^2}{E'} + \frac{2U_p^V}{B(W-a)} \frac{W}{r_p(W-a)} + a + z \qquad (4)$$

where U_p^V is the area under the load/mouth-opening displacement curve. Both Eq. 3 and Eq. 4 were used to compute values of J.

The method used to detect the onset of stable crack growth was the double displacement method. Both the mouth-opening displacements, V, and the load-line displacements, q, from each test were stored on a magnetic disk. The

derivatives dq/dV and d^2q/dV^2 were computed and plotted against V. The critical displacement was inferred from these plots. This method is further described in Results and Discussion.

RESULTS AND DISCUSSION

Cleavage Fracture Toughness

The fracture toughness data for the lower shelf and transition region are summarized in Figs. 6 through 9. The critical values of CTOD and J along with the critical fracture event for each specimen are reported; δ_c and J_c are defined at the occurrence of unstable cleavage without prior stable crack growth. When cleavage is preceded by stable crack growth, δ_u and J_u are measured at the point of instability.

Figures 6 and 7 show that the ductile-to-brittle transition curves shift approximately 30°C as the specimen thickness increases from 13 to 38 mm. The thickest specimen produces the greatest of crack-tip-region constraint; constraint is the restriction of plastic flow by the surrounding elastic material. Constraint causes a triaxial stress state and raises the flow stress near the crack tip. This increase in flow stress tends to promote cleavage fracture (i.e., shift the transition curve to the right) since it is easier to reach the fracture stress.

Note that the thickest specimens (B = 38.1 mm) had slightly deeper cracks than the other two specimen geometries shown in Figs. 6 and 7. The deeper cracks were necessary to prevent the load on the thick specimens from exceeding the capacity of the test machine. These deeper cracks probably contributed to the shift in the transition curve to higher temperatures.

The influence of crack length on the ductile-to-brittle transition curve is shown in Figs. 8 and 9. The curves in Figs. 8 and 9 tend to shift to higher temperatures with increasing crack length. Deeper-notched specimens (i.e., shorter ligament length) apparently have more crack-tip constraint. The data for the deep-notched geometry ($a/W \sim 0.75$) behave in an unusual manner. The curve fitted to these data (Figs. 8 and 9) crosses the curve representing the $a/W \sim 0.5$ data. At low values of δ_c and J_c, where the plastic zone is relatively small, the deep-notched geometry has more constraint than the $a/W \sim 0.5$ geometry. At higher temperatures (and higher δ_c and J_c values), the plastic zone at fracture is on the order of the size of the ligament in the deep-notched geometry. The constraint is relaxed as the plastic zone approaches a free surface.

In general, the transition shifts to higher temperatures with increasing thickness-to-ligament ratio, B/(W-a). For the five SENB geometries used in this investigation, B/(W-a) varied from 0.62 to 4.0; this corresponds to approximately a 40°C shift in the ductile-to-brittle transition.

The effect of ligament length on the slip patterns in SENB specimens was investigated. Two specimens were coated on one side with a photoelastic material that, when viewed with polarized light, changes color with strain. Black and white photographs of the multicolor strain patterns on two SENB specimens at net-section yield are shown in Fig. 10. The slip lines on both specimens emanate from the crack tip at initial angles of approximately 45° from the crack plane. These slip lines are then deflected inward by the bending stresses. At the neutral axis the normal stress changes sign; the portion of the ligament below the hinge point is in compression. In the deep-notched specimen (Fig. 10b), the hinge point is closer to the crack tip. The compressive stress field near the crack tip tends to produce additional

constraint. As ligament length decreases, the compressive stress field moves closer to the crack tip and constraint increases. As stated before, for very short ligaments constraint can be relaxed by plastic flow to the nearest free surface.

Increasing geometrical constraint causes the load at net-section yield to increase. This elevation of yield load can be quantified by the notch constraint factor, L, which is defined by the limit load expression for SENB specimens:

$$P_y = \frac{L\sigma_o(W-a)^2B}{4W} \qquad (5)$$

where P_y is the load at net-section yield. In the absence of a crack, L = 1.

Dimensionless load is plotted versus mouth-opening displacement in Figs. 11 and 12. Dimensionless load (i.e., load normalized for yield stress and ligament dimensions) is defined on the ordinates of Figs. 11 and 12 and is equal to L when $P = P_y$. The curves in Fig. 11, which are for a constant geometry at various temperatures, form a single curve because load is normalized for yield stress. Figure 12 shows that dimensionless load is elevated when crack length, specimen thickness or both are increased. The curves in Fig. 12 support the hypothesis that the observed shifts in the ductile-to-brittle transition curves (Figs. 6 through 9) are caused by increases in stress triaxiality.

Upper Shelf (Initiation) Toughness

During a fracture test with an SENB specimen, the load-line displacement, q, was continuously plotted against crack-mouth opening displacement, V.

After net-section yield, the q-versus-V plot is a nearly straight line. However, as the crack grows this line gradually decreases in slope because the center of rotation moves during crack growth. Figure 13 is a plot of the first derivative of q with respect to V plotted against V. The behavior at the far left of this plot represents the transition from elastic to plastic deformation. During plastic deformation, the first derivative remains relatively constant and then increases sharply. At V = 1.48 mm there is a sharp drop in the first derivative. This behavior is characteristic of fracture tests where tearing was observed. Observation of fracture surfaces of specimens that fractured prior to and immediately following the onset of tearing and the corresponding derivative plots indicate that the sharp drop in the first derivative coincides with incipient tearing. At higher displacements the curve has a zig-zag shape, which is believed to be associated with successive increments of crack growth.

Figure 13 is typical of the first derivative plots from fracture tests in which tearing was observed. The spike in the curve, which was taken as the point of incipient tearing, is slightly more pronounced than the other spikes. Often the initiation point is ill defined because of the uncertainty of which spike corresponds to the onset of stable crack growth.

The critical displacement V_i and the corresponding area under the curve were used to compute δ_i and J_i from Eqs. 1 and 3. Figures 14 and 15 show values of δ_i and J_i, respectively, for the five SENB specimen geometries. Both J_i and δ_i are apparently independent of geometry and δ_i is approximately independent of temperature. J_i increases slightly with decreasing temperature because the area under a load-displacement curve at a constant displacement increases with increasing flow stress. Owing to the uncertainty in this

technique, the point of incipient crack growth is often not well defined, contributing to the scatter seen in Figs. 14 and 15.

The Rotational Factor

The rotational factor, r_p, is defined as the distance from the crack tip to the hinge point divided by the ligament length. The rotational factor was previously defined in Eq. 2, where r_p is expressed as a function of specimen dimensions and the plastic components of mouth-opening (V_p) and load-line (q_p) displacements [14]. Equation 2 was derived assuming the SENB specimen deforms in pure bending about a hinge point; the specimen halves are assumed to remain rigid.

The rotational factor was measured for five geometries of ABS EH36 steel SENB specimens at various temperatures. Figure 16 shows that r_p is insensitive to geometry and test temperature. The mean value of the data in Fig. 16 is 0.522; the standard deviation is 0.030.

Equation 6 can be used to determine the sensitivity of CTOD measurements to variations in r_p [14]:

$$\frac{d(\delta p/Vp)}{dr_p} = \frac{(a+z)\ (W-a)}{[r_p(W-a)+a+z]^2} \qquad (6)$$

Using r_p = 0.5, W = 25.4 mm, a = 12.7 mm and z = 1.3 mm, the above derivative is equal to 0.43. The value of r_p recommended by the British Standard [1] is 0.4, or 20 percent below the nominal value of 0.5 for this specimen material. If 0.4 is used in Eq 1, a 14 percent error in the computed CTOD value would occur. It is therefore important to have a reasonably accurate estimate of r_p for a given material; the standard value (0.4) is apparently not adequate for all materials.

Estimation of J from CMOD

For deep-notched SENB specimens, the J-integral is usually estimated from Eq 3. The value of J can also be estimated from the load-versus-mouth-opening displacement curve using Eq. 4. Equation 4 is based on the Sumpter and Turner [15] equation, although they approximated the plastic area under the P/V curve by

$$U_p^V \cong P_L V_p \tag{7}$$

where P_L is the limit load.

The J-integral was calculated for a number of tests using Eqs. 3 and 4, and the agreement is very good. Figure 17 shows a comparison of estimates from the two equations. The data represent a single specimen at various displacements. The differences between the two J estimates for this particular specimen range from 0.5 to 1.5 percent.

The value of r_p used in Eq 4 to generate Fig. 17 was measured from the same specimen using Eq 2. The excellent agreement between Eqs. 3 and 4, as shown in Fig. 17, is evidence that the simple hinge mechanism is an adequate model to describe the plastic deformation of an SENB specimen. Figure 17 also shows that the J-integral can be accurately measured from the mouth-opening displacement if r_p is known. Thus, it is possible to measure both J and CTOD from an SENB specimen with a single clip gage.

Relationships Between J and CTOD

Under conditions of small-scale yielding the relationship between J and CTOD can be estimated by

$$J = m\sigma_o\delta \tag{8}$$

where m is a dimensionless constant that relates J to CTOD and yield stress; m = 1 for plane stress and m = 2 for plane strain. The value of m for large-scale yielding should lie between 1.0 and 2.0.

The plastic term in Eq 4 is similar to the equation for the plastic CTOD:

$$\delta_p = \frac{r_p(W-a)V_p}{r_p(W-a) + a + z} \tag{9}$$

From Eqs 4 and 9 one can obtain a simple equation for the ratio of the plastic J to the plastic CTOD

$$\frac{J_p}{\delta_p} = \frac{2U_p^V W}{V_p B r_p (W-a)^2} \tag{10}$$

Equation 10 has been incorporated into a computer program that plots J_p/δ_p as a function of mouth-opening displacement. A typical plot is shown in Fig. 18. The ratio J_p/δ_p increases with displacement because of work hardening. The work hardening can be accounted for by replacing the yield stress in Eq 8 with a nominal flow stress:

$$J_p = m_p \sigma_{flow} \delta_p \tag{11}$$

The nominal flow stress can be estimated by

$$\sigma_{flow} = \frac{\bar{P}}{P_y} \sigma_o \tag{12}$$

where P is the average load defined as

$$\bar{P} = \frac{U_p^v}{V_p} \tag{13}$$

and P_y is the load at yield defined previously in Eq. 5.

Combining Eqs. 5 and 10 through 13 yields the following relationship for m_p.

$$m_p = \frac{L}{2r_p} \tag{14}$$

For the ABS grade EH36 steel, $r_p \cong 0.5$; therefore, $m_p \cong L$ (the notch constraint factor). Thus, the relationship between plastic components of J and CTOD (Eq. 11) depends on the geometrical constraint of the specimen and the flow properties of the material.

The η Factor

The η factor is a dimensionless constant that relates J to energy divided by ligament area. It is used in a more general form of Eq. 3:

$$J = \frac{\eta U}{B(W-a)} \tag{15}$$

where $\eta \cong 2$ for deep notched SENB specimens. The above equation can be divided into elastic and plastic components [15]:

$$J = \frac{\eta_e U_e}{B(W-a)} + \frac{\eta_p U_p}{B(W-a)} = \frac{K^2}{E'} + \frac{\eta_p U_p}{B(W-a)} \tag{16}$$

The elastic η factor, η_e, can be derived from the elastic compliance and stress intensity coefficient. The solid line in Fig. 19 is a plot of η_e versus notch depth [16].

Since J can be defined as the negative of the spatial derivative of work, the plastic η factor, η_p, or the overall η factor, η_o, can be computed as follows:

$$J = \frac{\eta_o U}{B(W-a)} = \frac{-1}{B}\frac{dU}{da} \tag{17}$$

hence

$$\eta_o = -\frac{(W-a)}{U}\frac{dU}{da} \tag{18}$$

A series of SENB specimens with notch depths ranging from a/W = 0.19 to 0.75 were tested at room temperature. The area under the load-versus-load-line displacement curve, U, was measured for each specimen at displacements of 1.0, 1.5, and 2.0 mm. These values of U were then plotted versus crack length, and dU/da was measured for various crack lengths by drawing tangents to the U-versus-a curves and computing the slopes; η_o was then computed as a function of crack length. The results are plotted in Fig. 19. According to Fig. 19, η_o is relatively independent of crack length down to a/W = 0.19. It therefore seems reasonable to use a value of η_o = 1.8 - 2.0 for all J measurements from SENB specimens with $a/W \geq 0.2$. A variation of 0.10 in η_o corresponds to approximately a 5 percent error in the measured value of J.

SUMMARY AND CONCLUSIONS

The fracture toughness (critical J and CTOD) of structural steels in the ductile-to-brittle transition region is dependent on size and geometry. The transition can be shifted to higher temperatures by increasing the thickness or decreasing the ligament length of SENB specimens, or both. These transition shifts are attributed to increases in crack-tip region constraint that elevate the flow stress locally. This elevation of the flow stress tends to promote cleavage fracture since it is easier to reach the fracture stress. Fracture toughness in the transition region is geometry dependent; one cannot safely predict the fracture behavior of a large structure from the toughness of a small specimen.

The rotational factor, r_p, in SENB specimens is insensitive to geometry and temperature. Significant errors in CTOD may result if the standard r_p value (0.4) is used for all materials. Both J and CTOD can be measured from an SENB specimen with a single clip gage at the crack mouth. The relationship between J and CTOD is a function of specimen geometry. The η factor is approximately equal to 1.85 for SENB specimens with a/W ranging from 0.19 to 0.75.

ACKNOWLEDGMENTS

This research was funded by the U.S. Department of Interior Minerals Management Service. The contract monitor was Mr. John B. Gregory.

REFERENCES

[1] British Standard 5762: Methods for Crack Opening Displacement (COD) Testing, 1979, The British Standards Institution, London.

[2] M. G. Dawes, The Welding Institute Research Bulletin, 13, 1982, p. 50.

[3] M. G. Dawes, ASTM STP 668, 1979, p. 307.

[4] A. B. Stuber, Ph.D. Thesis, University of Kansas, 1980.

[5] R. O. Ritchie, R. F. Smith, and J. F. Knott, Metal Science, 9, 1975, p. 485.

[6] A. Penelon, M. N. Bassim, and J. M. Dorlot, ASTM STP 677, 1979, p. 449.

[7] I. Milne, Mat. Sci. Eng., 30, 1977, p. 243.

[8] G. G. Chell and G. M. Spink, Eng. Frac. Mech., 9, 1977, p. 101.

[9] I. Milne and P. J. Worthington, Mat. Sci. Eng., 26, 1976, p. 185.

[10] G. G. Chell and A. Davidson, Mat. Sci. Eng., 24, 1976, p. 45.

[11] G. G. Chell and R. S. Gates, Int. J. Fract., 14 (2), 1978, p. 223.

[12] P. M. S. T. deCastro, J. Spurrier, and P. Hancock, ASTM STP 677, 1979, p. 486.

[13] M. G. Dawes, The Welding Institute Research Bulletin, 7, 1976, p. 185.

[14] I.-H. Lin, T. L. Anderson, R. deWit and M. G. Dawes, Int. J. Fract., 20, 1982, p. R3.

[15] J.D.G. Sumpter and C. E. Turner, ASTM STP 601, 1976, p. 3.

[16] O. L. Towers, Welding Institute Report 136/1981, March 1981.

List of Figures

Fig. 17. Comparison of J estimates from Eqs. 3 and 4.

Fig. 18. The ratio of the plastic components of J and CTOD as a function of displacement.

Fig. 19. The overall η factor (η_0) as a function of a/W and displacement. The elastic η factor curve [16] is superimposed for comparison.

Table 1. Chemical Composition of the ABS Grade EH36 Steel (Weight Percent)

C	Mn	P	S	Si	Cu	Ni	Cr	Mo	Fe
0.12	1.39	0.015	0.006	0.380	0.05	0.03	0.05	0.007	bal.

Table 2. Test Matrix for Fracture Toughness Tests on SENB Specimens

	B = 12.7 mm	B = 25.4 mm	B = 38.1 mm
a/W = 0.2	X	X	X
a/W = 0.5		X	
a/W = 0.75		X	

W = 25.4 mm (1.0 in)

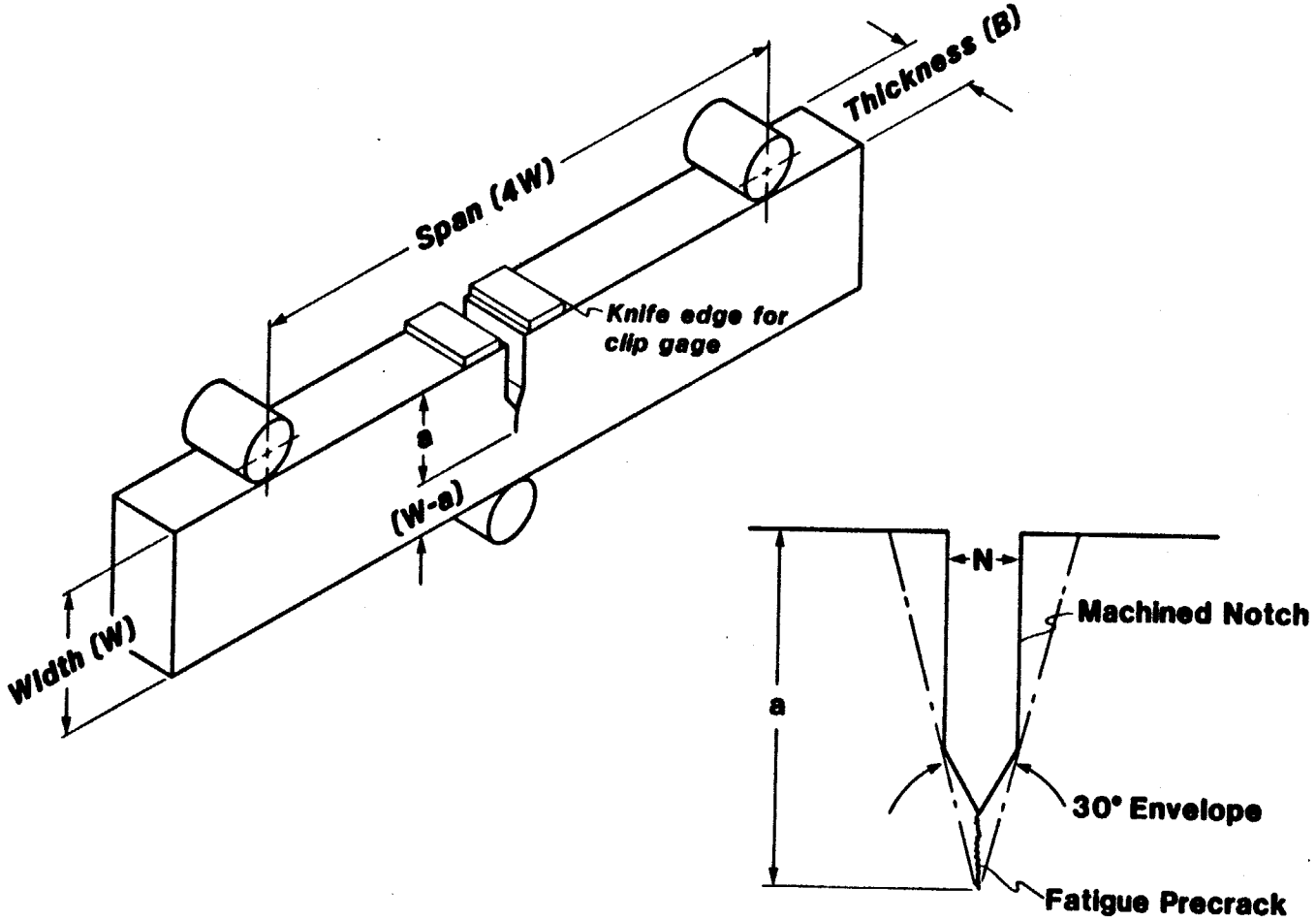

Fig. 1. Three-point bend specimen used to obtain fracture toughness test results.

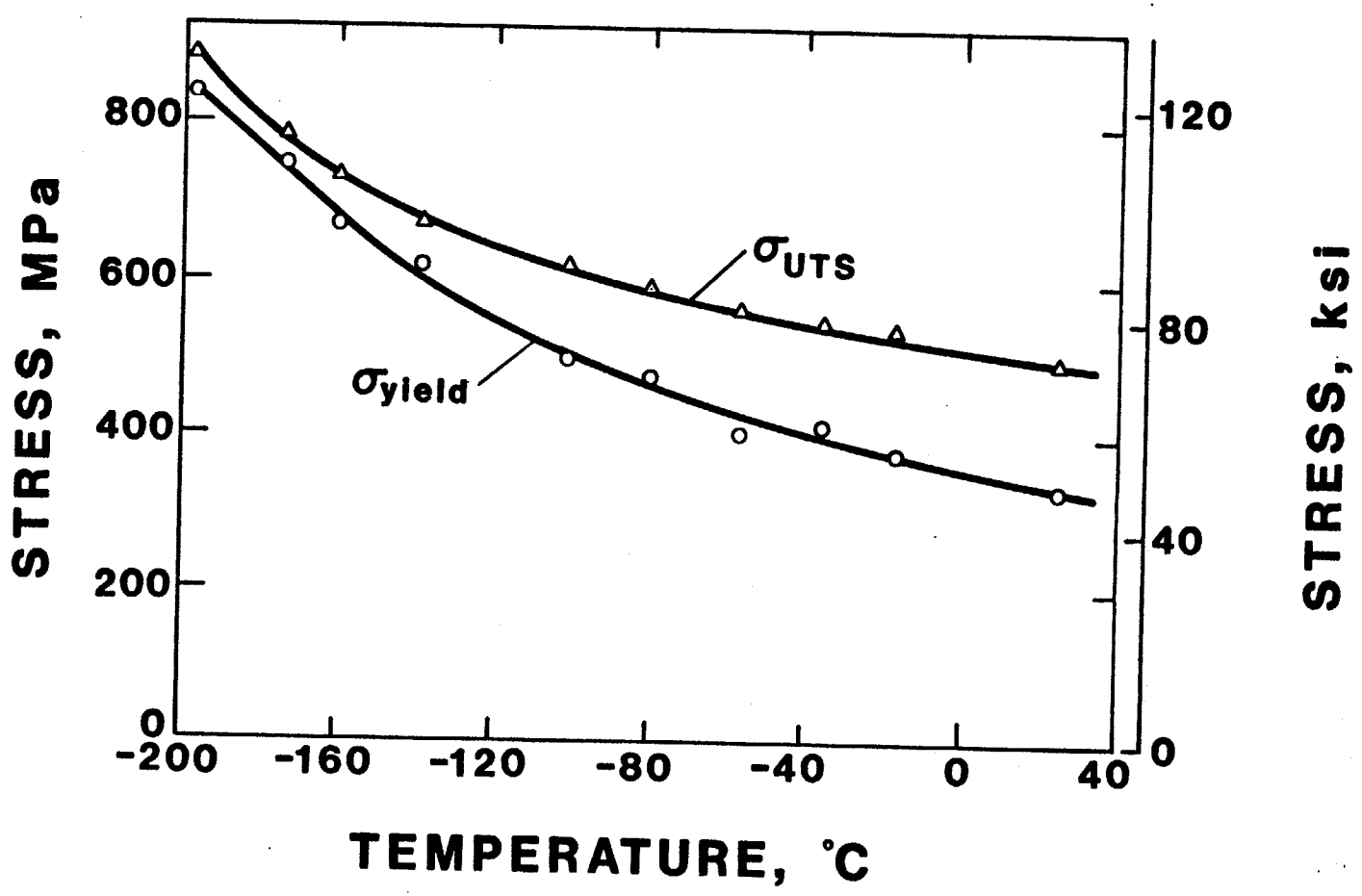

Fig. 2. Tensile properties of ABS grade EH36 steel as a function of temperature.

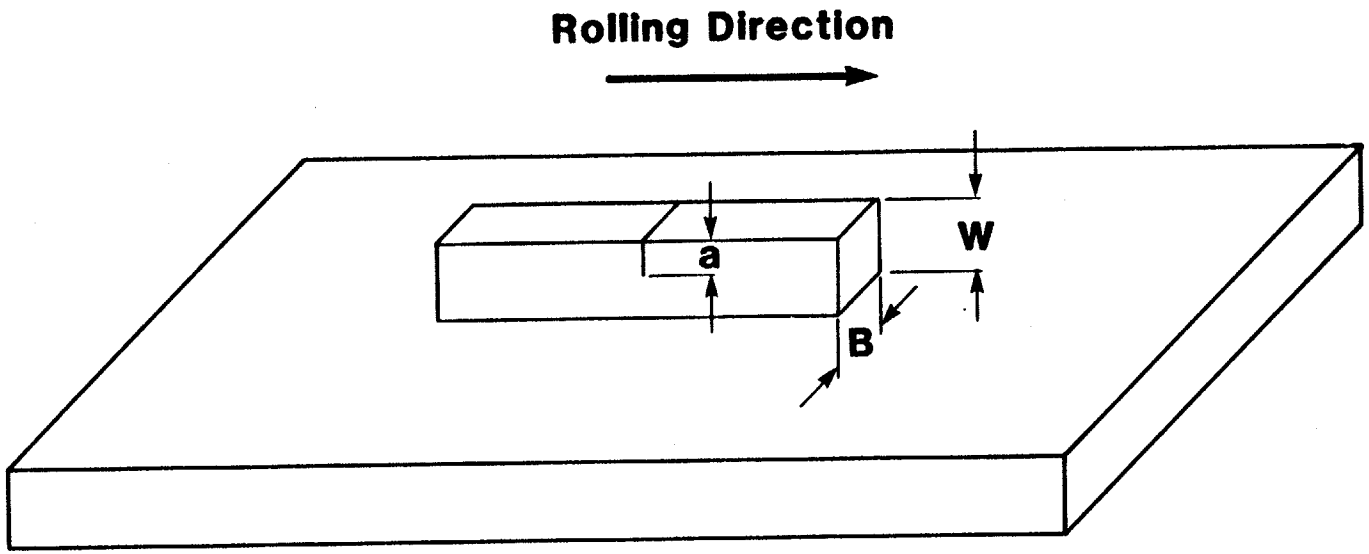

Fig. 3. Orientation of SENB specimens with respect to the rolling direction. Charpy impact specimens were also prepared with this orientation.

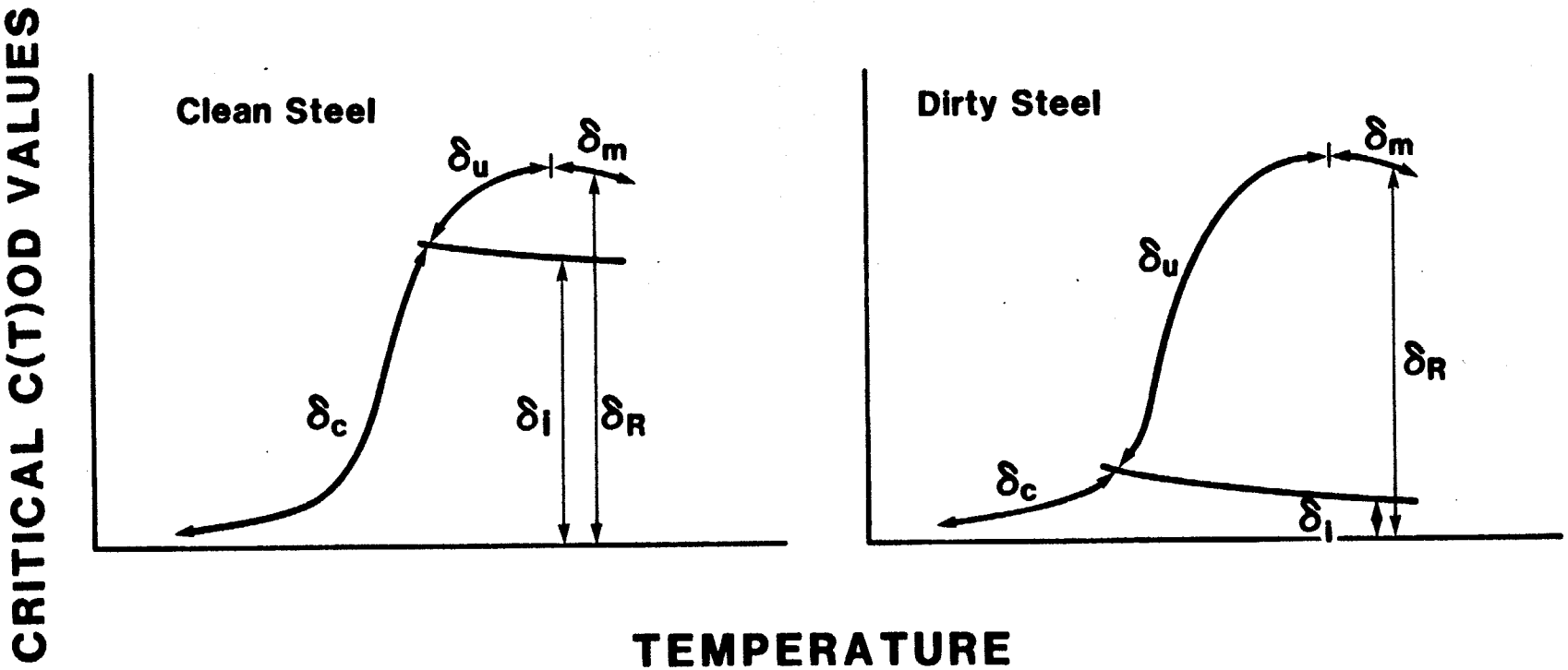

δ_c = Unstable cleavage-no prior slow crack growth

δ_u = Unstable cleavage-with prior slow crack growth

δ_m = Plastic collapse or tearing instability

δ_I = Onset of slow stable crack growth

δ_R = Resistance curve value

Fig. 4. Notation for critical CTOD values [1].

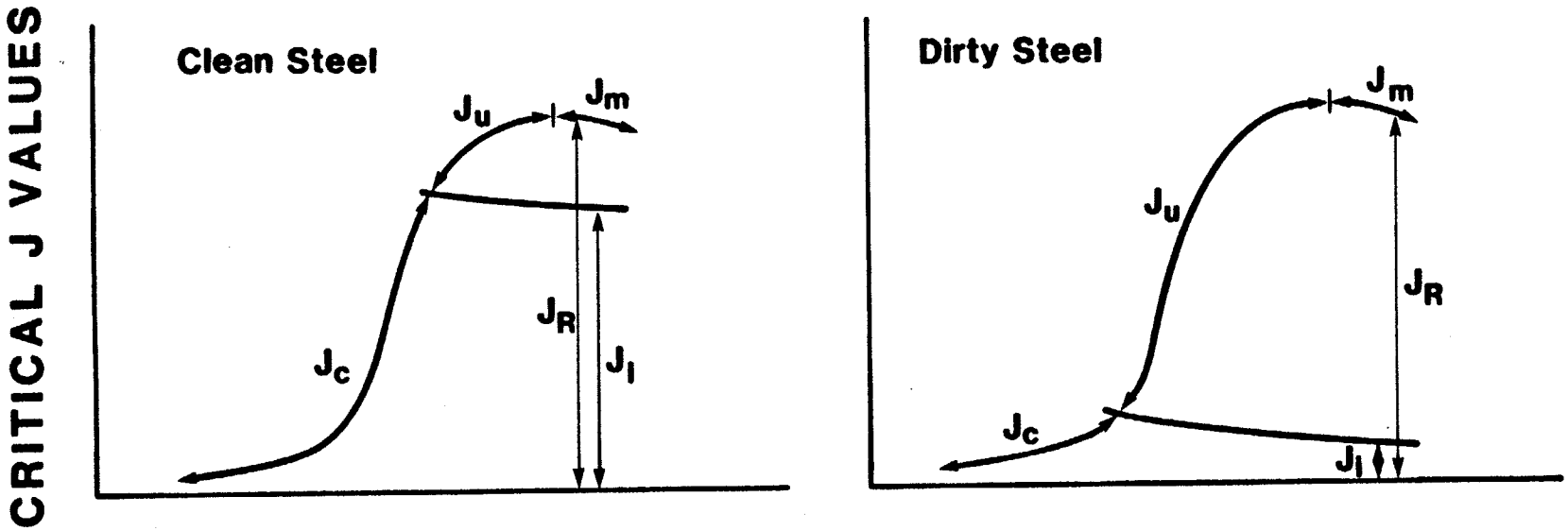

J_c = Unstable cleavage-no prior slow crack growth

J_u = Unstable cleavage-with prior slow crack growth

J_m = Plastic collapse or tearing instability

J_I = Onset of slow stable crack growth

= J_{Ic} when certain conditions are met

J_R = Resistance curve value

Fig. 5. Notation for critical J values [2].

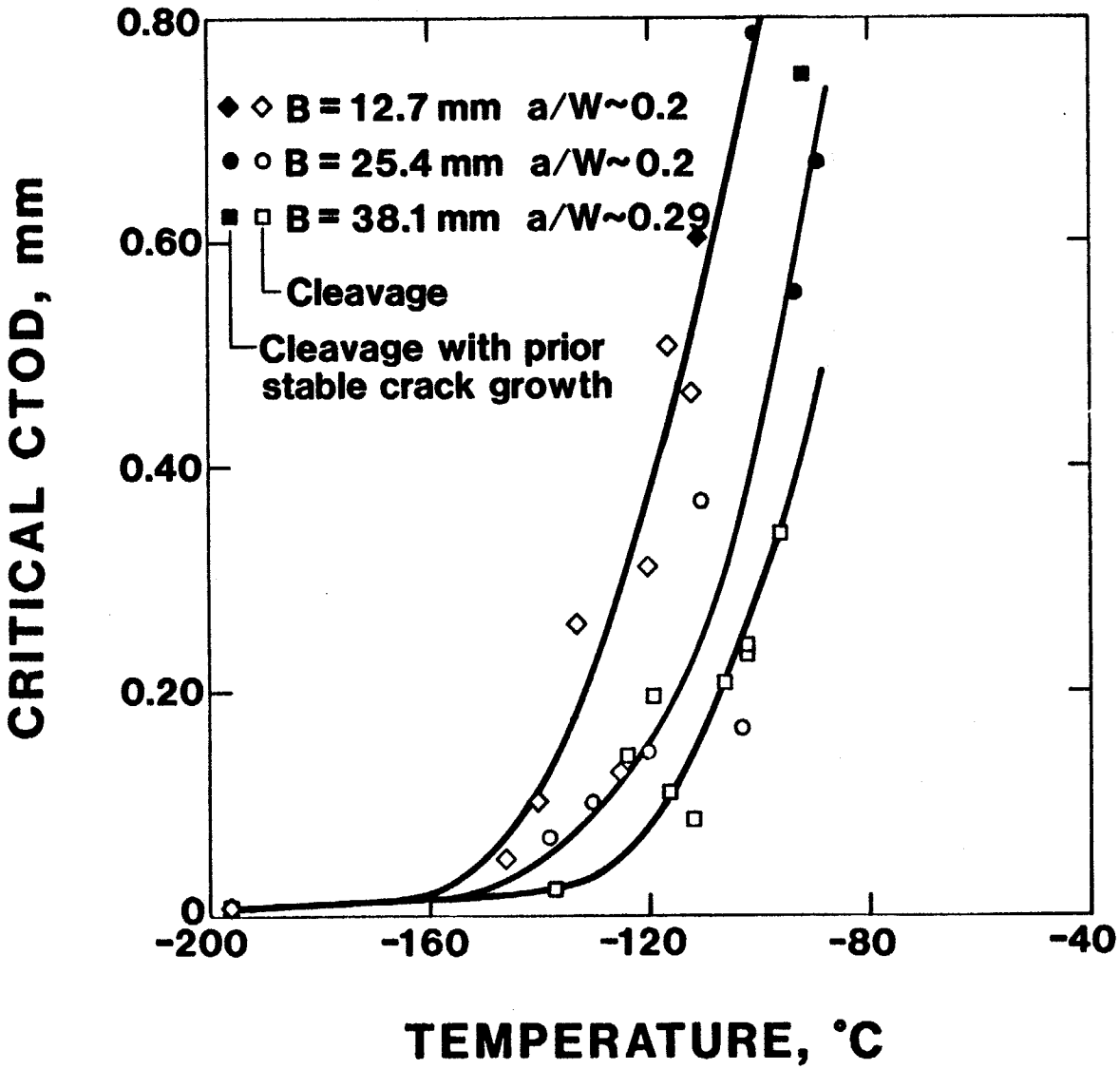

Fig. 6. Critical CTOD for cleavage as a function of temperature and specimen thickness for ABS grade EH36 steel. W = 25.4 mm (1.0 in).

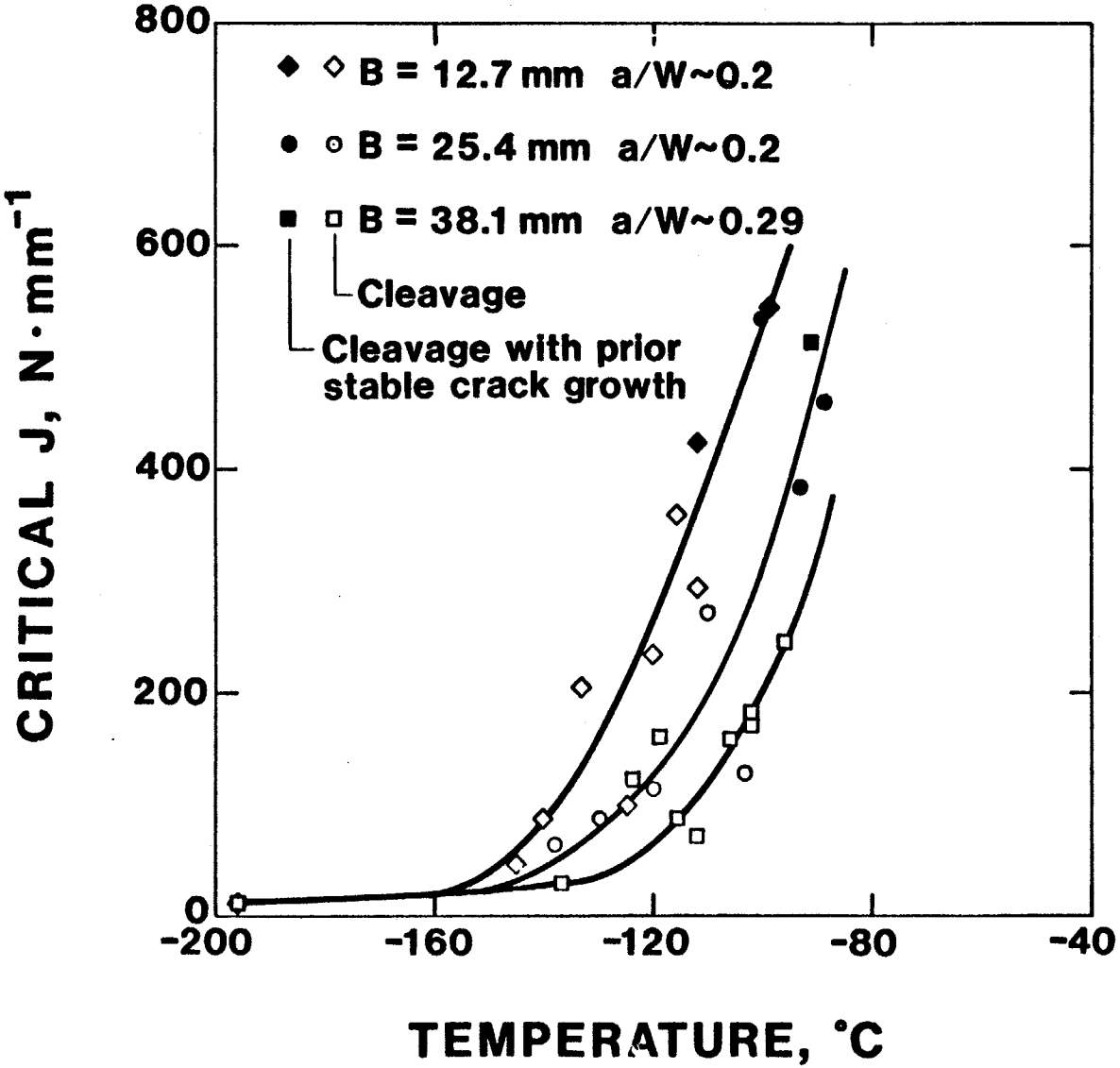

Fig. 7. Critical J for cleavage as a function of temperature and specimen thickness for ABS grade EH36 steel. W = 25.4 mm (1.0 in).

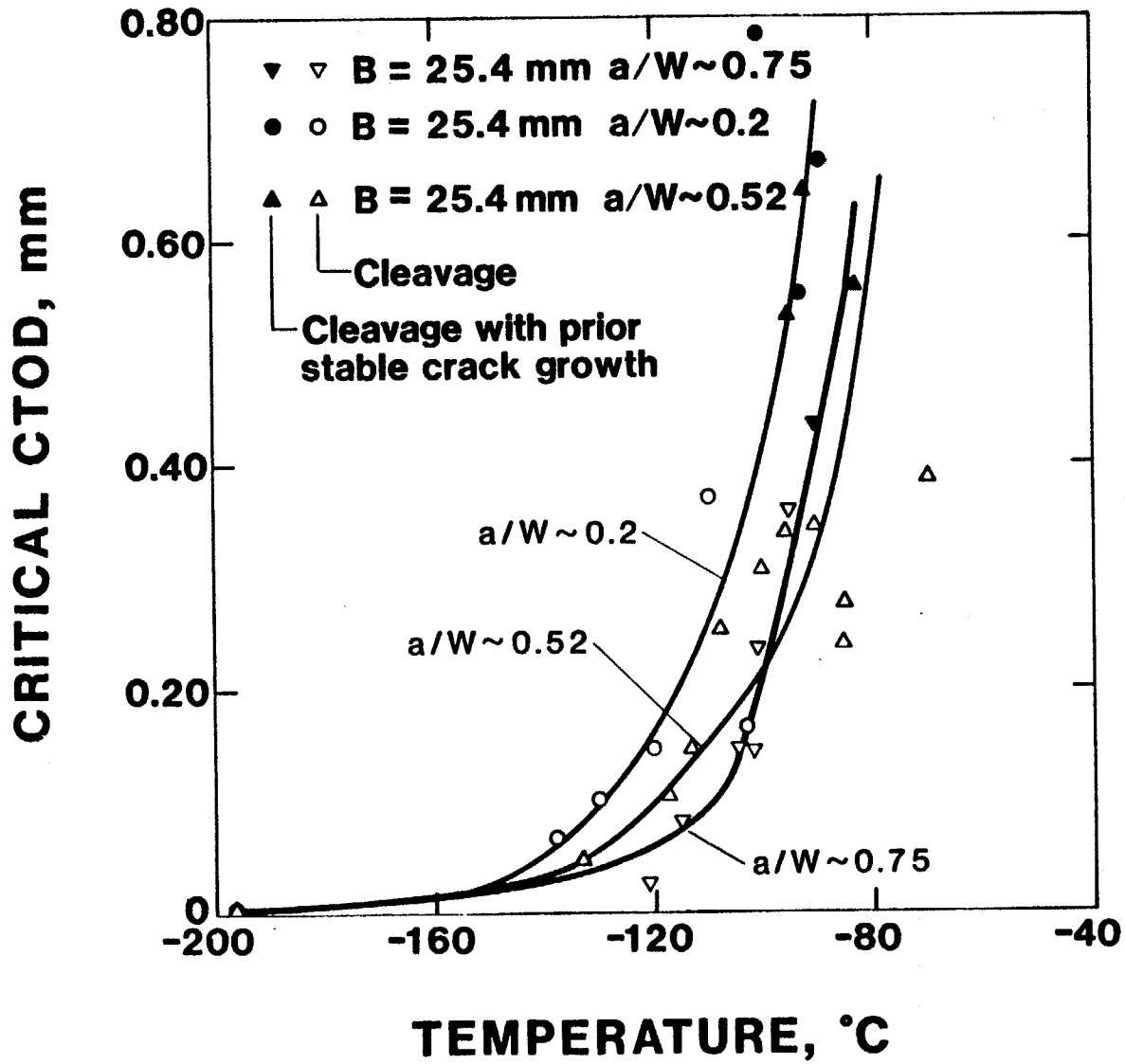

Fig. 8. Critical CTOD for cleavage as a function of temperature and crack length for ABS grade EH36 steel. W = 25.4 mm (1.0 in).

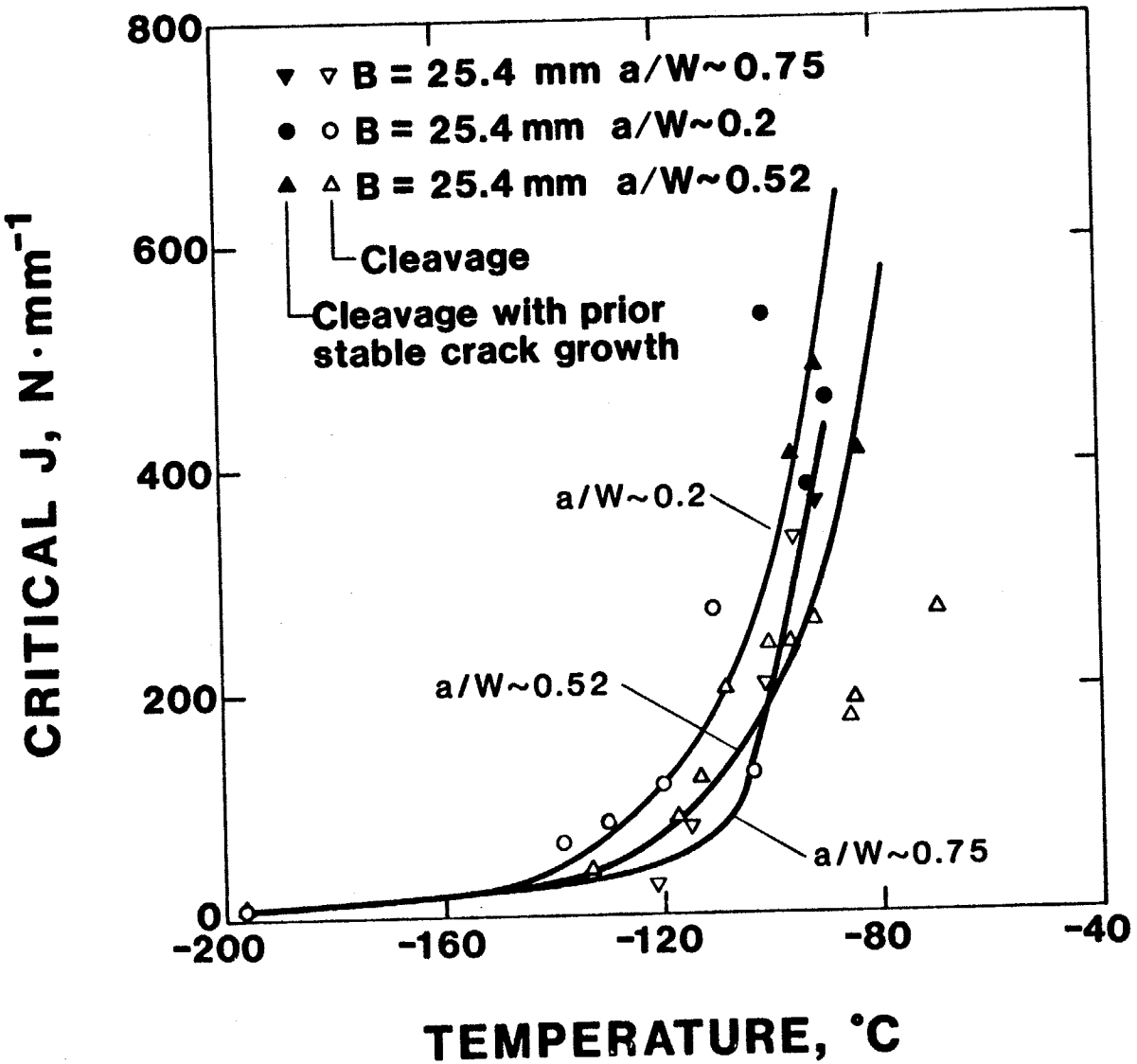

Fig. 9. Critical J for cleavage as a function of temperature and crack length for ABS grade EH36 steel. W = 25.4 (1.0 in).

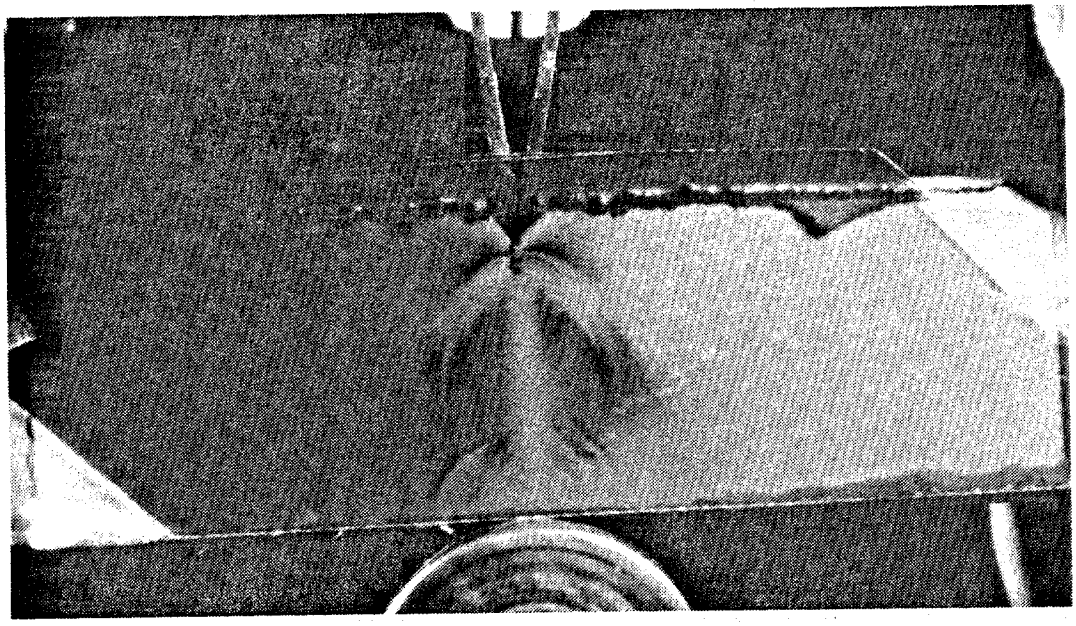

(a)

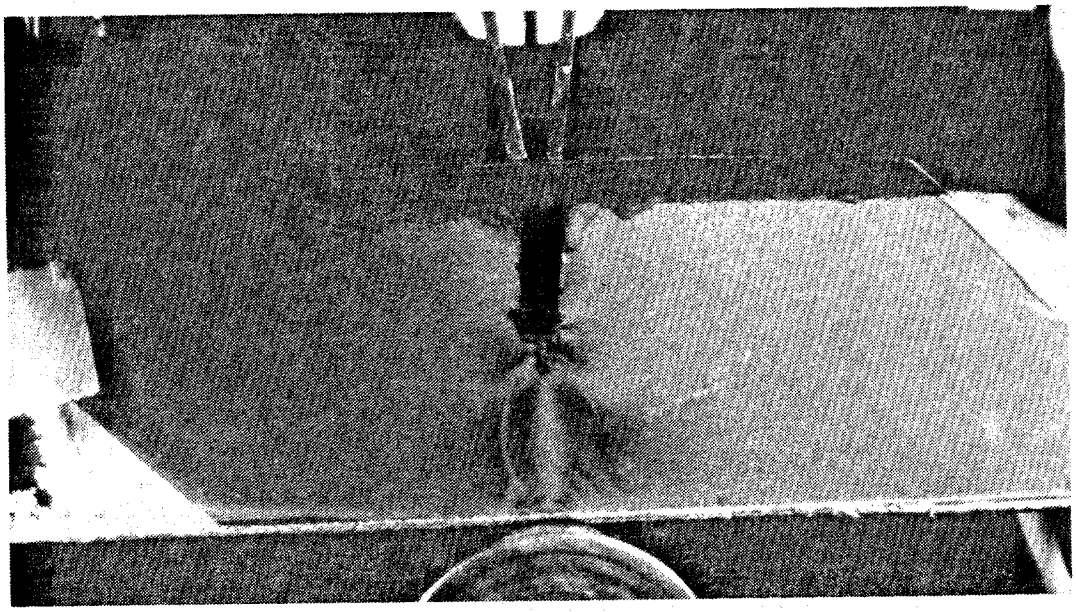

(b)

Fig. 10. Photoelastic strain patterns for SENB specimens; a) a/W ~ 0.2, b) a/W ~ 0.5.

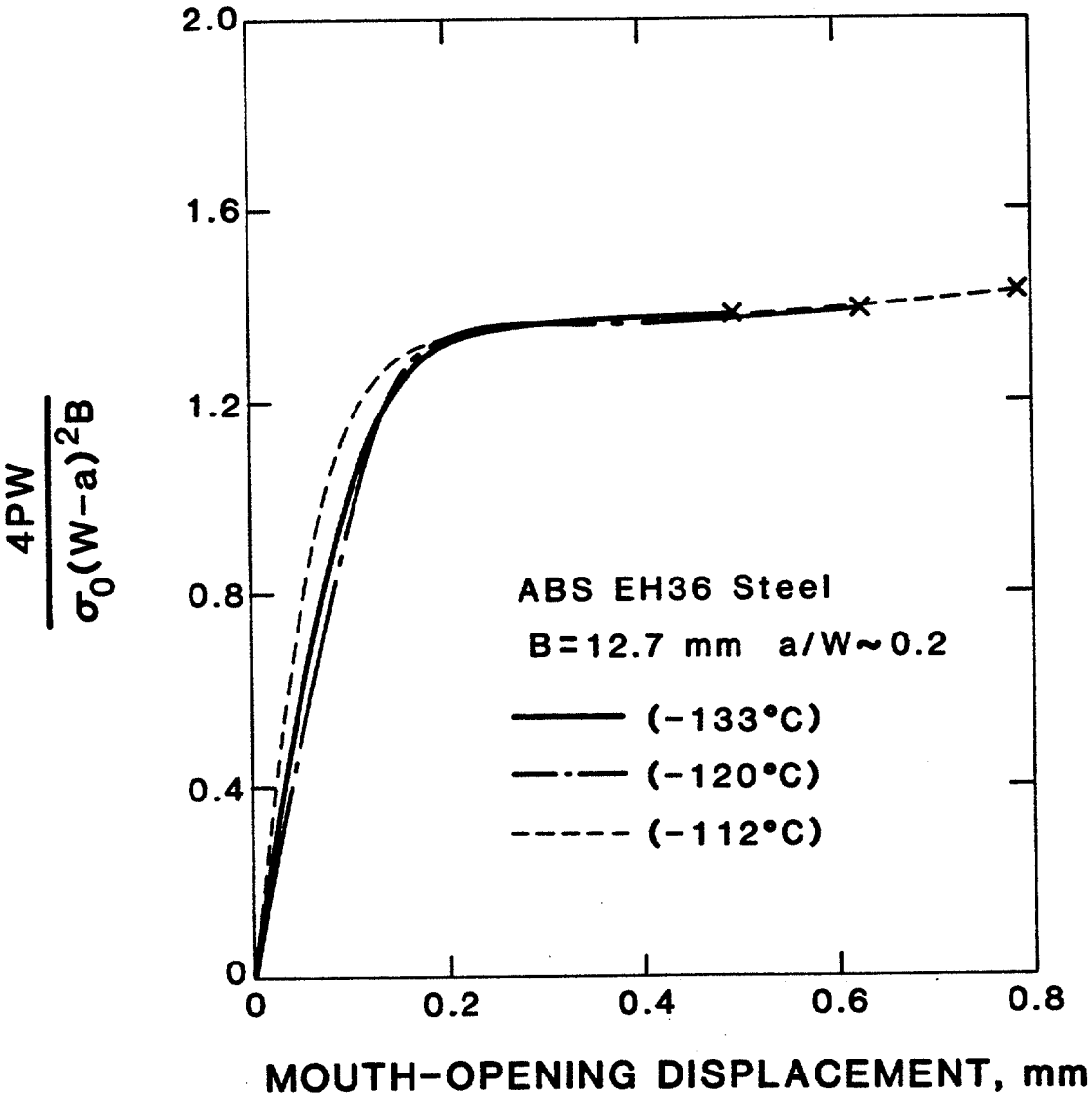

Fig. 11. Nondimensional-load-versus-displacement curves at various temperatures for a constant SENB specimen geometry.

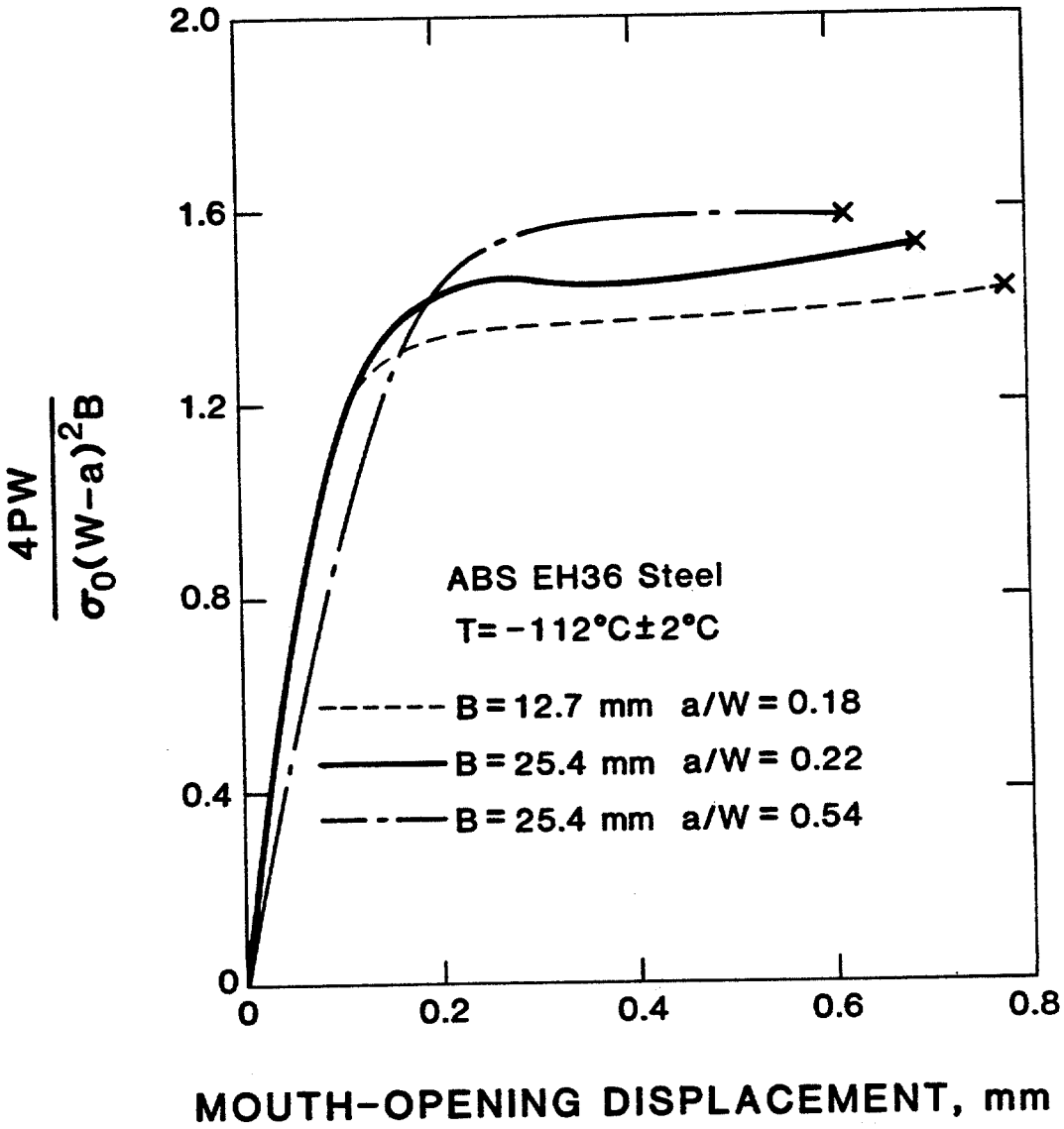

Fig. 12. Nondimensional-load-versus-displacement curves as a function of SENB specimen geometry.

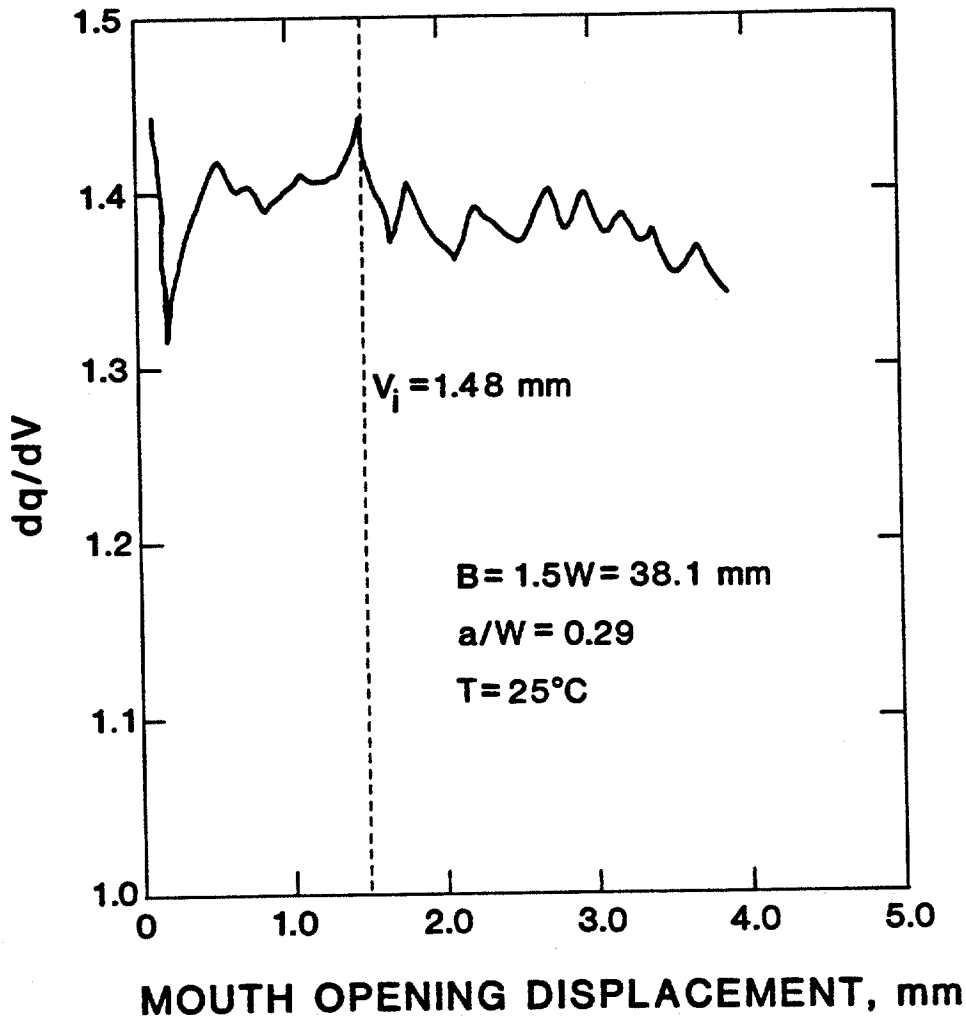

Fig. 13. Derivative of q with respect to V. A sharp drop in the first derivative generally indicates tearing.

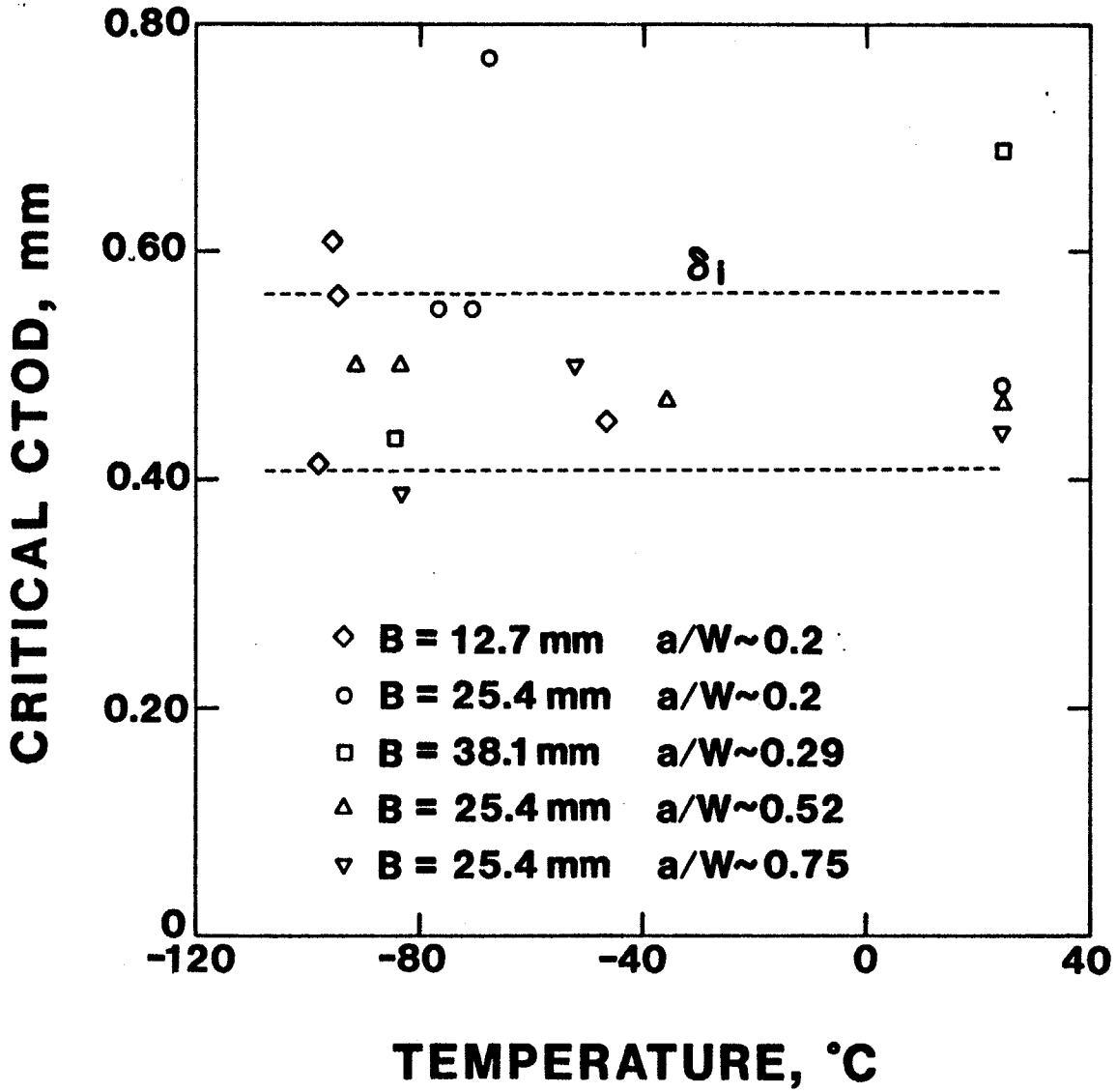

Fig. 14. Critical CTOD for the onset of tearing as a function of temperature and SENB specimen geometry for ABS grade EH36 steel. W = 25.4 mm (1.0 in).

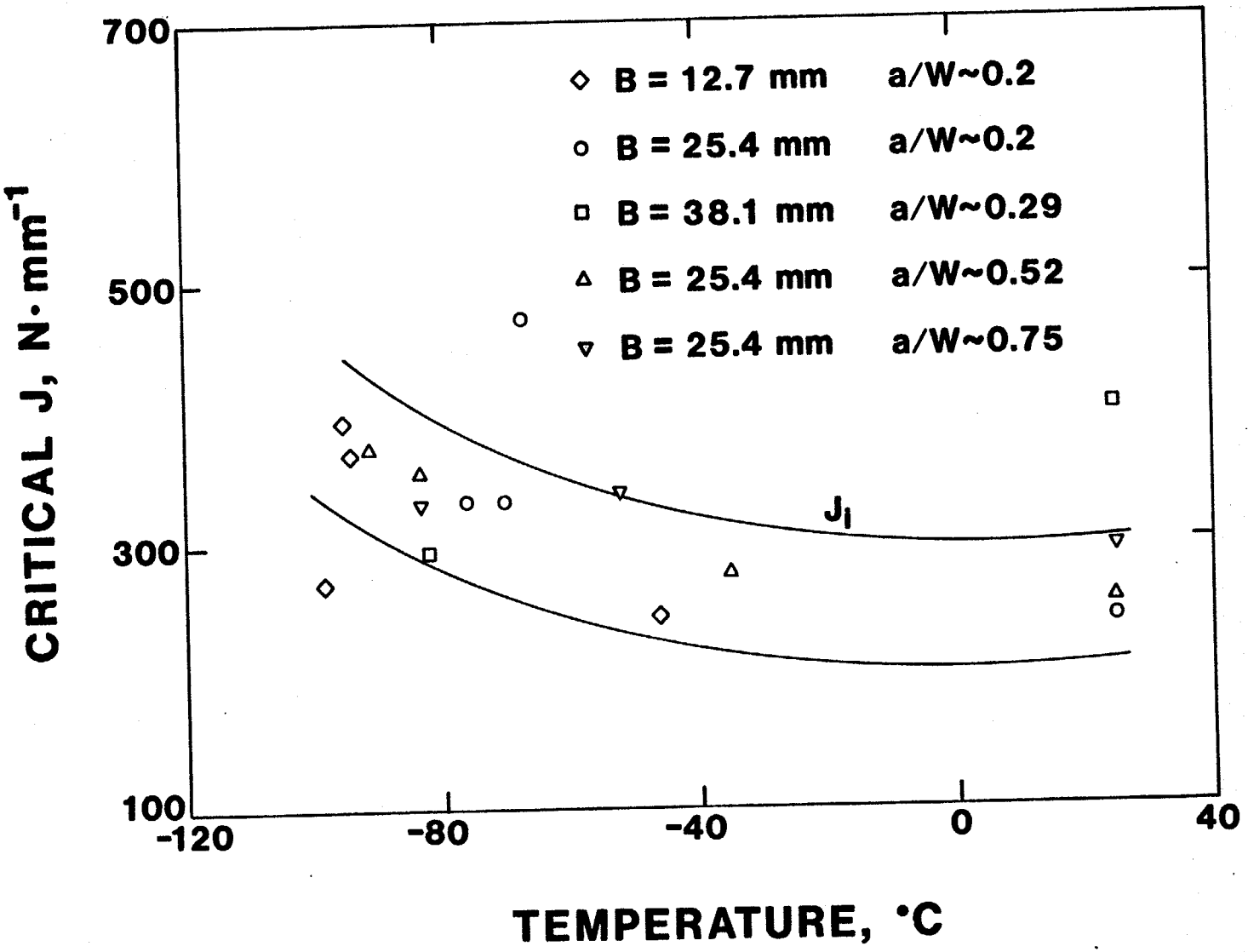

Fig. 15. Critical J for the onset of tearing as a function of temperature and SENB specimen geometry for ABS grade EH36 steel. W = 25.4 mm (1.0 in).

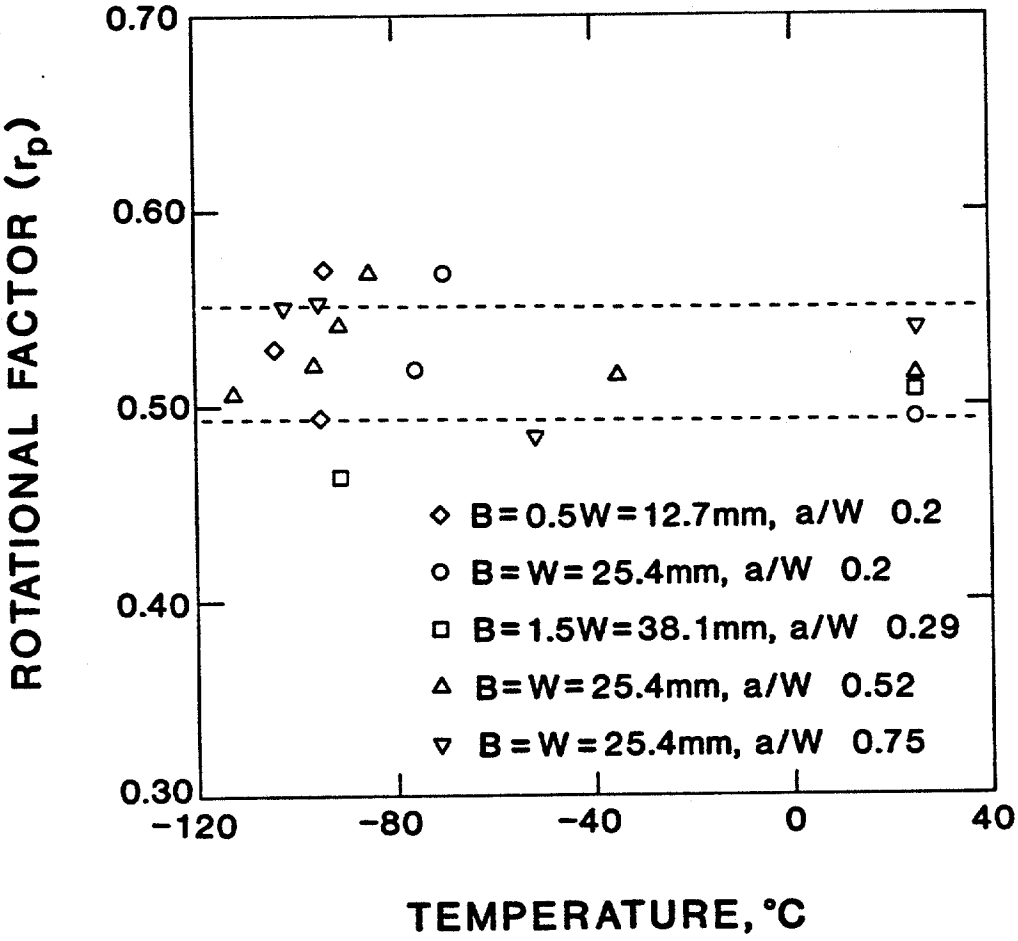

Fig. 16. Plastic rotational factor as a function of SENB specimen geometry and temperature for ABS grade EH36 steel.

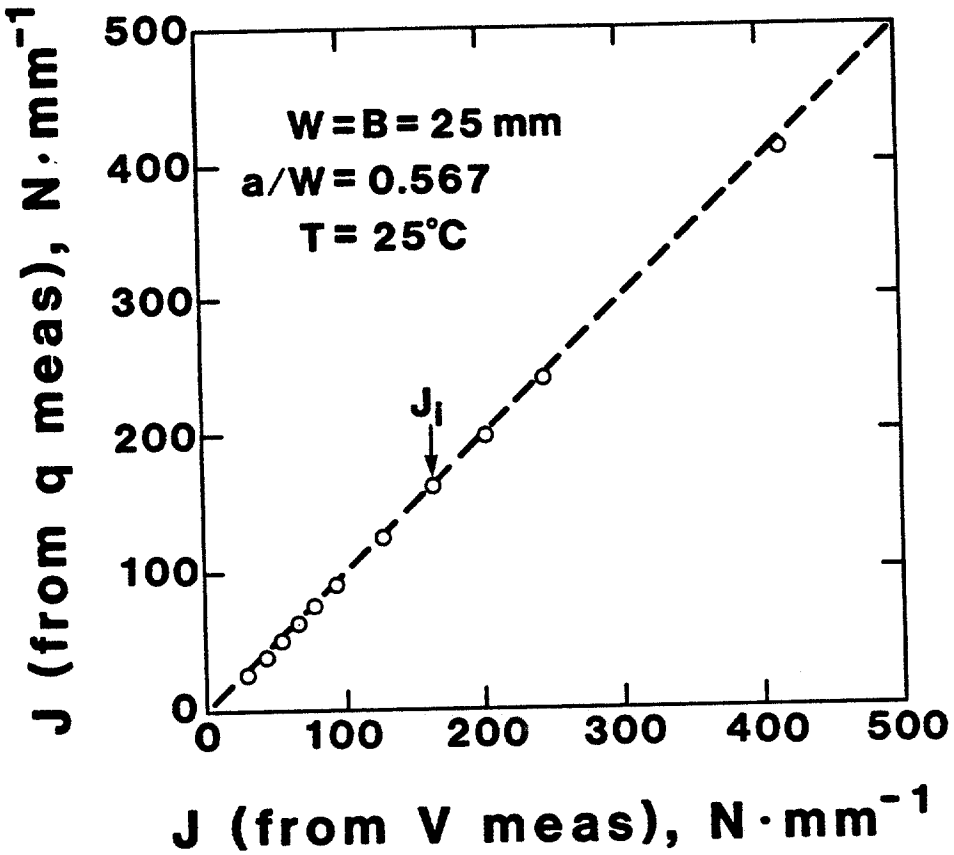

Fig. 17. Comparison of J estimates from Eqs. 3 and 4.

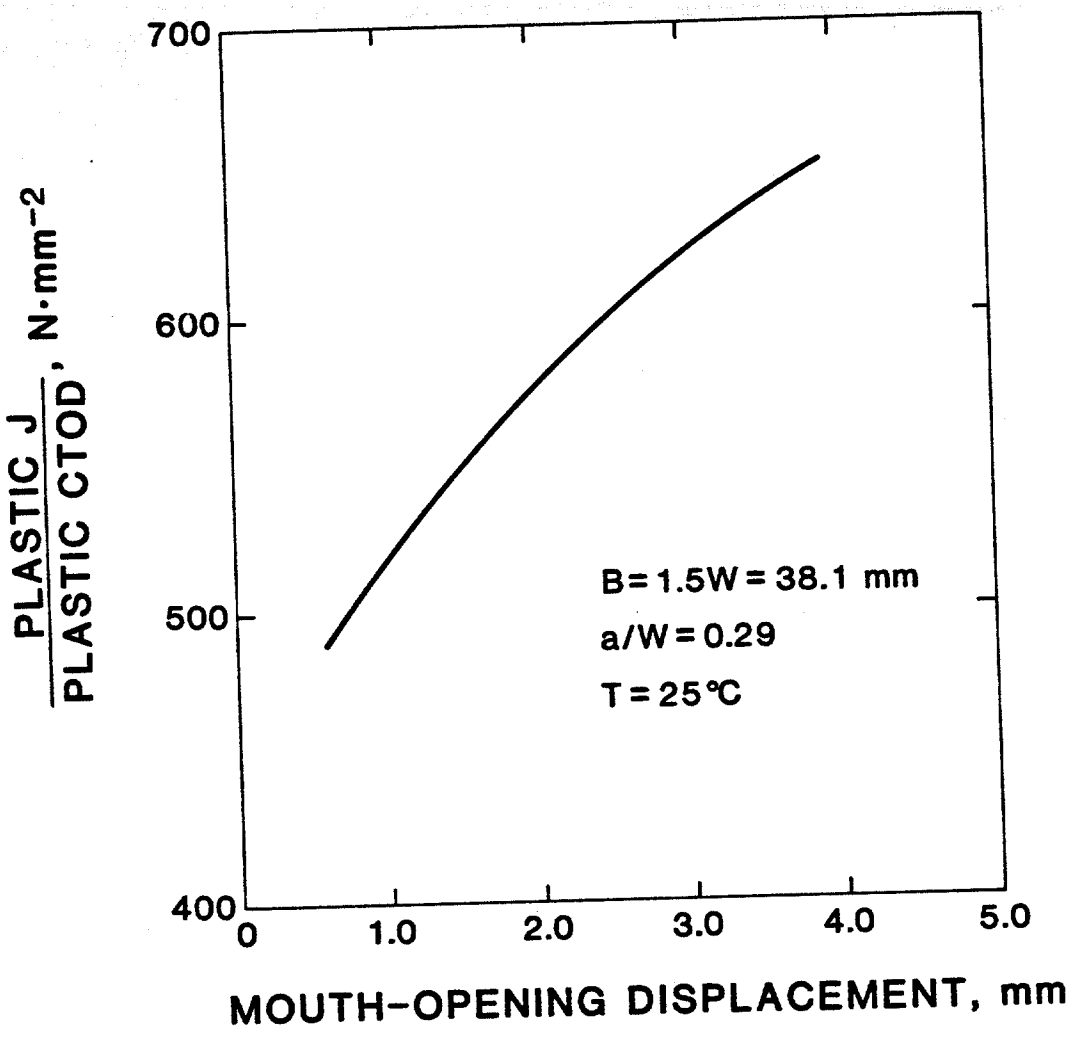

Fig. 18. The ratio of the plastic components of J and CTOD as a function of displacement.

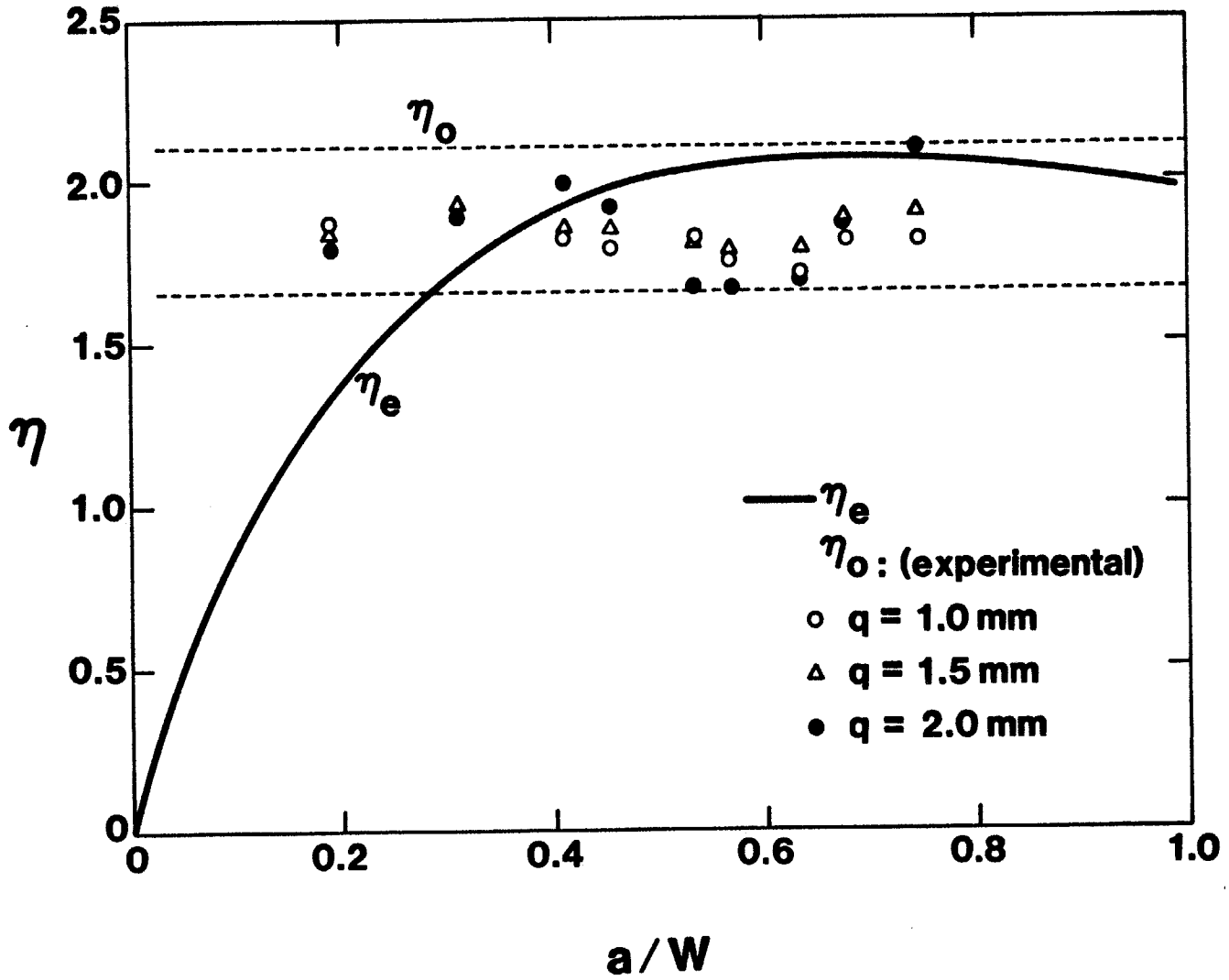

Fig. 19. The overall η factor (η_o) as a function of a/W and displacement. The elastic η factor curve [16] is superimposed for comparison.